Interleaved Bidirectional DC-DC Converter for Renewable Energy Application based on a Multiple Storage System

Yehya I. Mesalam
Department of Industrial Engineering, College of Engineering, Northern Border University, Saudi Arabia | Industrial Engineering Department, Faculty of Engineering, Zagazig University, Egypt
yehya.mesalam@nbu.edu.sa | ymesalam@yahoo.com

Shaaban Awdallh
Department of Electrical Engineering, College of Engineering, Northern Border University, Saudi Arabia | Department of Engineering Basic Science, Faculty of Engineering, Menoufia University, Egypt
shaban.awdallah@nbu.edu.sa

Hajer Gaied
National Engineering School of Gabes, University of Gabes, Tunisia
hajer.giaed@yahoo.fr

Aymen Flah
Processes, Energy, Environment, and Electrical Systems (code: LR18ES34), National Engineering School of Gabes, University of Gabes, Tunisia | MEU Research Unit, Middle East University, Amman, Jordan | College of Engineering, University of Business and Technology (UBT), Jeddah 21448, Saudi Arabia | Private Higher School of Applied Sciences and Technologies of Gabes, University of Gabes, Tunisia | Applied Science Research Center, Applied Science Private University, Amman, 11931, Jordan
flahaymening@yahoo.fr (corresponding author)

Received: 21 January 2024 | Revised: 30 January 2024 | Accepted: 7 February 2024

 DOI: https://doi.org/10.48084/etasr.6944

ABSTRACT

Due to its fewer components, the DC-DC three-phase converter has a simpler design and could be less expensive. However, it can present challenges in terms of precise voltage regulation and current balancing, due to the limited number of switching phases. On the other hand, the three-phase converter offers more precise voltage regulation and improved current balance owing to its higher number of phases. Although this results in increased design complexity and potentially higher cost, it allows for a more uniform distribution of current load among MOSFETs. The particular needs of the application, acceptable trade-offs between complexity, cost, and performance, as well as the requirement for precise voltage regulation and ideal current balancing, can determine which option is the best. This work investigates a three-phase interlaced DC converter with a parallel MOSFET. A two-way DC-DC converter was used to assess PWM when charging and discharging a battery. The results demonstrate a great DC voltage gain without a very high cycle load.

Keywords-interleaved bidirectional DC-DC converter; parallel-connected MOSFET; buck-boost DC-DC converter; battery storage; SOC

I. INTRODUCTION

DC-DC converters must be used in renewable energy applications to successfully incorporate renewable energy sources into power systems. Some significant state-of-the-art parts for DC-DC converters in this industry are listed in [1-2]. Voltage conversion is necessary to integrate photovoltaic solar panels into the electrical grid, even though they generate constant voltage. DC-DC converters, such as buck or boost converters, regulate the voltage of solar panels according to the requirements of the system. To optimize conversion efficiency, DC-DC converters also employ advanced techniques such as Maximum Power Point Tracking (MPPT) [3]. DC-DC converters, like batteries, are also utilized in energy storage systems to manage charge, discharge, and voltage conversion. These converters help optimize battery charging/discharge efficiency, control voltage, and manage compatibility with the rest of the system [4-12]. Therefore, DC-DC converters play an essential role in renewable energy applications by allowing efficient conversion and control of DC voltage generated by renewable energy sources, integrating energy storage systems, and optimizing energy system performance.

Research and development in this area focus on improving energy efficiency, miniaturizing converters, and integrating renewable energy sources into power systems. The interlaced DC-DC converter, often referred to as the cross-switched DC-DC converter, is one kind of uninsulated converter implemented to change a DC voltage from one level to another. Its primary function is to alter the voltage of a DC power source to satisfy the demands of an electronic system. In summary, an interlaced DC-DC converter is an electronic device that efficiently converts continuous voltage from one level to another, using two synchronized conversion stages to improve energy efficiency and overall system performance. Thus, the usage of interlaced DC-DC converters in renewable energy applications offers certain advantages, namely better energy efficiency, managing energy source variability, integration of several renewable sources, accurate voltage regulation, reduced system size and weight, and increased reliability. These benefits contribute to a more efficient and reliable use of renewable energy in a variety of applications.

Advances in technology have led to a greater dependence on electrical products for daily needs. Achieving sustainable growth in society and the economy requires striking a balance between energy use and environmental conservation more than ever. This study combines a control strategy designed for DC-DC converters with a short conversion period. Changes made on the input immediately affect the output sides of converters, since there is no galvanic isolation between the input and output sides in a non-isolated converter architecture. The non-isolated converter topology has fewer components than the isolated one. However, non-isolated converters have a few minor issues that require attention, such as excessive duty cycle ratio, insufficient voltage gain, and additional circuitry for optimal operation. There are differences between each category of converter topology advantages and disadvantages. The application requirements are the basis for the decision. This study investigated some recently published studies on interleaved DC-DC converters. Previous studies examined the applications of conventional DC-DC converters in renewable energy applications, their limitations, and recent developments. However, they did not discuss the available control techniques for the operation of DC-DC converters [13]. An interleaved DC-DC converter converts a direct voltage from one level to another while reducing power losses and improving exit voltage stability.

The terminal voltages of renewable energy sources are usually low and change over time. Therefore, to offer reliable electrical energy, it is a standard procedure to interface with the DC bus using a bidirectional DC-DC converter with a high conversion ratio. The converter must lower the load current to ensure smooth power transfer, but this has the unexpected consequence of restricting power capacity during conversion. This study also evaluates energy conversion between operating modes to offer a rapid energy conversion method.

II. THE BIDIRECTIONAL DC-DC INTERLEAVED CONVERTER OF PARALLEL CONNECTED MOSFET

The elevating converter is one converter type that is most frequently used to charge or discharge batteries due to its wide conversion range and user-friendliness [14-15]. This kind of converter allows the battery voltage levels to be adjusted to the DC bus voltage levels by maintaining a steady voltage and controlling the disruptions caused by connecting and disconnecting loads and energy sources. However, the battery receives a ripple in the switch's current, which leads to power losses and battery deterioration. When utilizing *N* phases made up of semiconductors and filter components, the output power can even get close to tenths of kilowatts. Reduced filter element dimensions arise from the operating frequency, becoming an integer multiple of the switching frequency. A straightforward solution for the application covered in this study is the typical interleaved bidirectional DC-DC converter. Figure 1 depicts a three-phase topology, with V1 and V2 standing for the DC link and the SC, respectively. Moreover, I1 and I2 are the corresponding currents across the SC and the DC link, whereas $P_1 = V_1 \times I_1$, and the same applies to the second phase power.

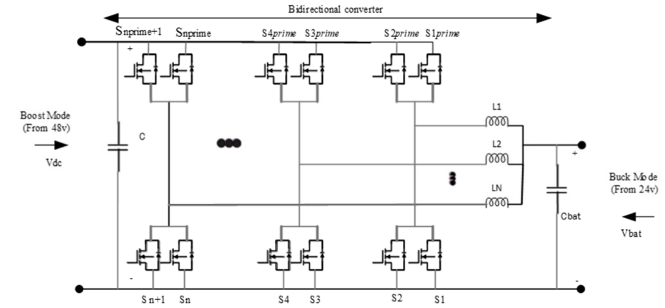

Fig. 1. Interleaved bidirectional DC-DC converter.

This study describes a qualitative and quantitative examination of the interleaved bidirectional DC-DC converter, which has four switches in each arm divided into lower-group and upper-group switches [16-19]. Figure 2 illustrates the three-phase interleaved bidirectional DC-DC converter employing *n* parallel-connected MOSFETs. Eight power switches ($S_{(1...6)}$ and $S_{(1prime...6prime)}$) and three inductors make up the power circuit (L1, L2, L3). The parasitic resistances, such as inductor resistances (RL1, RL2, RL3) and switch resistances, are considered to derive the non-ideal DC voltage gain (RS1). When the suggested converter runs in step-up mode (boost), where DH is the duty cycle of the gate signals S1-S6, energy passes from the battery to the DC bus side. The step-down mode (buck) transfers energy from the DC bus to the battery side, with DL being the duty cycle of the gate signals S_{1prime}-S_{6prime}. The main waveforms for the duty cycle range belonging to [0, 0.25] follow.

A. Boost Mode: First Stage [t_0-t_1]

S_1, S_{4prime}, S_{3prime}, S_6 are turned on, and S_{1prime}, S_{2prime}, S_{5prime}, S_{6prime}, S_3, S_4, S_5 are turned off. Inductors L_1 and L_3 start storing energy from the battery through S_1 and S_6 at this point, and its current, $I_{L1}(t)$, $L_3(t)$ increases linearly until t_1. Since the voltages v_{bat} and v_{bat} - v_{DC} are applied to L_1, L_2, and L_3, respectively, current $I_{L2}(t)$ continues to fall linearly and the stored energy in L_2 is given to the load through S_{3prime} and S_{4prime}. The total of $I_{L1}(t)$ and $I_{L2}(t)$ equals the battery current $I_{bat}(t)$). Equations (1)-(3) can be used to calculate the instantaneous currents.

$$I_{L1}(t) = I_{L1}(t_0) + \left(v_{bat} - \frac{I_{bat}}{3}(R_{L1} + R_{s1})\right).\frac{(t-t_0)}{L_1} \quad (1)$$

$$I_{L2}(t) = I_{L2}(t_0) + \left(v_{DC} + \frac{R_{L2}.I_{bat}}{3} + \frac{R_{S_{4prime}}.I_{bat}}{8} - v_{bat}\right).\frac{(t-t_0)}{L_2} \quad (2)$$

$$I_{L3}(t) = I_{L3}(t_0) + \left(v_{bat} - \frac{I_{bat}}{3}(R_{L3} + R_{S6})\right).\frac{(t-t_0)}{L_3} \quad (3)$$

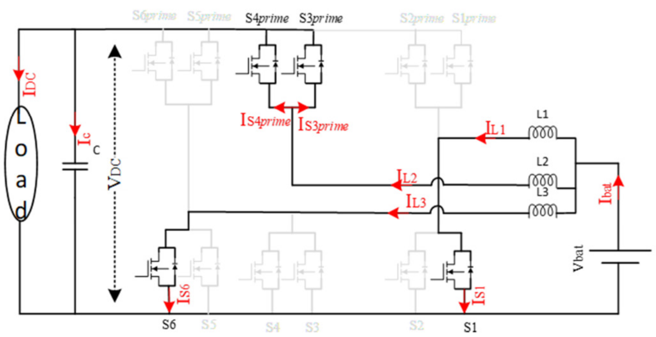

Fig. 2. Equivalent circuits of boost mode using three-phase interleaved converter.

B. Boost Mode: Second Stage [t_1-t_2]

S_1, S_2, S_3, S_4, S_5, and S_6 are turned off, and S_{1prime}, S_{2prime}, S_{3prime}, S_{4prime}, S_{5prime}, and S_{6prime} are turned on. Through S_{1prime}, S_{2prime}, S_{3prime}, S_{4prime}, S_{5prime}, and S_{6prime}, both conductors now send energy to the load. Then, both conductors receive the voltage v_{bat} - v_{DC}. As a result, the instantaneous voltage equations for L_1, L_2, and L_3 are shown in (4)-(6), and the current across all inductors falls linearly.

$$v_{L1}(t) = v_{bat} - v_{DC} - I_{bat}\left(\frac{R_{L1}}{3} + \frac{R_{S_{2prime}}}{8}\right) \quad (4)$$

$$v_{L2}(t) = v_{bat} - v_{DC} - I_{bat}\left(\frac{R_{L2}}{3} + \frac{R_{S_{3prime}}}{8}\right) \quad (5)$$

$$v_{L3}(t) = v_{bat} - v_{DC} - I_{bat}\left(\frac{R_{L3}}{3} + \frac{R_{S_{6prime}}}{8}\right) \quad (6)$$

Buck mode features eight steps in one switching time and two operation regions, just like the boost mode. The circuit is symmetric, so just the fourth period is examined. The main waveforms for the duty cycle range that belongs to [0, 0.25] follow.

C. Buck Mode: First Stage [t_0-t_1]

S_3, S_4, S_{1prime}, and S_{5prime} are turned on, S_{3prime}, S_{4prime}, S_1, S_2, S_{2prime}, S_{6prime}, S_5 , and S_6 are turned off. As energy from the v_{DC} is stored through the inductor L_1, its current $I_{L1}(t)$ grows linearly until t_1. The voltage v_{DC} - v_{bat} and v_{bat} is delivered to L_1, L_2, and L_3, and the current $I_{L2}(t)$ continues to fall linearly. As a result, the stored energy in L_2 is transferred to the load through S_3 and S_4. Equations (7)-(9) can be used to calculate the instantaneous currents and voltages of L_1, L_2, and L_3.

$$I_{L1}(t) = I_{L1}(t_0) + \left(v_{DC} - v_{bat} - I_{DC}\left(R_{L1} - R_{S1prime}\right)\right).\frac{(t-t_0)}{L_1} \quad (7)$$

$$I_{L2}(t) = I_{L2}(t_0) - \left(v_{bat} + (I_{bat} - I_{DC}).\left(R_{L2} + \frac{R_{S4}}{2}\right)\right).\frac{(t-t_0)}{L_2} \quad (8)$$

$$I_{L3}(t) = I_{L3}(t_0) + \left(v_{DC} - v_{bat} - I_{DC}(R_{L3} - R_{S5prime})\right).\frac{(t-t_0)}{L_3} \quad (9)$$

D. Buck Mode: Second Stage [t_1-t_2]

S_3, S_4, S_1, S_2, S_5, and S_6 are turned on, S_{3prime}, S_{4prime}, S_{2prime}, S_{1prime}, S_{5prime}, and S_{6prime} are turned off, as shown in Figure 3. Through *S3*, *S1*, *S2*, and *S4*, both conductors now deliver energy to the load. Then, both conductors receive the voltage -v_{bat}. As a result, the instantaneous current/voltage equations for *L1*, *L2*, and *L3* are shown in (10)-(12), and the current through all inductors falls linearly.

$$I_{L1}(t) = I_{L1}(t_1) - \left(v_{bat} + I_{bat}\left(\frac{R_{L1}}{3} + \frac{R_{S2}}{8}\right)\right).\frac{(t-t_1)}{L_1} \quad (10)$$

$$I_{L2}(t) = I_{L2}(t_1) - \left(v_{bat} + I_{bat}\left(\frac{R_{L2}}{3} + \frac{R_{S3}}{8}\right)\right).\frac{(t-t_1)}{L_2} \quad (11)$$

$$I_{L3}(t) = I_{L3}(t_1) - \left(v_{bat} + I_{bat}\left(\frac{R_{L3}}{3} + \frac{R_{S5}}{8}\right)\right).\frac{(t-t_1)}{L_1} \quad (12)$$

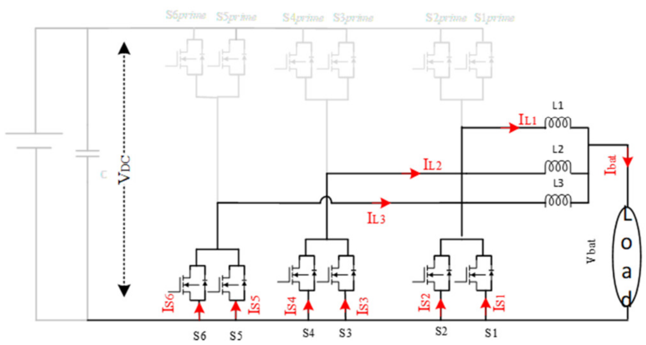

Fig. 3. Equivalent circuits of buck mode using the three-phase interleaved converter.

III. TECHNIQUE AND CONTROL STRATEGY

Only the functions of the variables that need to be controlled are employed in the system transfer functions that may be obtained from this state space. The control structure illustrated in Figure 4 is used to regulate the bus voltage and lower the battery's current ripple [19], where it is evident that measuring the three system status variables is required. Two PI controllers are used to control the charging and discharging of batteries: one generates reference current based on the mode of operation (charging or discharging), and the other regulates the battery's current.

This case study includes two modes of operation:

- When the DC bus is connected and the battery's full voltage is reached at the control objective set point of the first PI closed loop, the charging mode switches to automated.
- Discharging mode: this mode is automatically triggered when the DC bus is disconnected, and the first PI closed loop's control purpose is to maintain a steady load voltage throughout the discharging process.

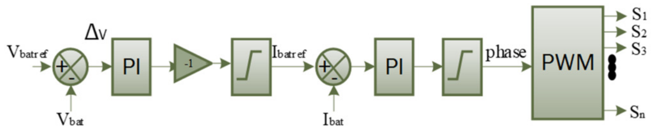

Fig. 4. Control system for the three-phase DC-DC converter.

IV. EXPERIMENTAL RESULTS

The measurements were performed using a battery-linked DC source to validate the functionality of PWM. The tests were configured with a fixed DC bus voltage v_{DC} = 48 V, a battery voltage v_{bat} = 24 V, f_{s1} = 10kHz, and a nominal power of 500 W, as displayed in Table I. The simulation results are shown for the case of two-phase and three-phase DC-DC converters.

TABLE I. PARAMETERS OF THE EXPERIMENTAL SYSTEM

Parameter	Specification
Inductor	57.6 10^{-3}H
Battery capacitor	50 Ah
Capacitor	1000 mF

A resistive charge of 4.4 Ω is connected as part of this operation, which simulates the converter during boost (discharge mode) on the low voltage side 24 V, 50 Ah battery, which is thought to be powered by the 48 V DC bus voltage. Comparably, the DC bus replacement resistive charge is connected to a 24 V, 50 Ah battery that is in charge of operation. The system is then simulated for buck operation mode, where the 24 V battery acts as a charge. Figures 5 and 6 demonstrate the comparison by the variation of the different battery initiation %SOC. A correct charging voltage is essential to prevent the battery from overloading or under-charging, which could damage the battery or reduce its capacity.

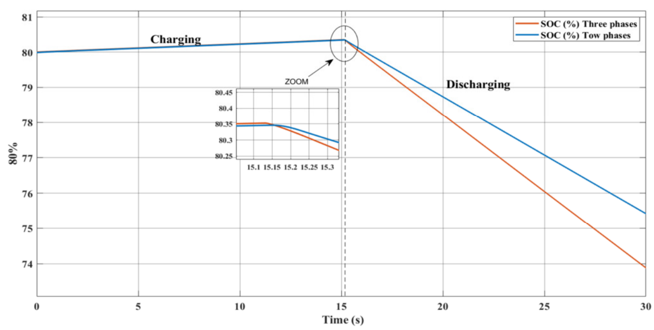

Fig. 5. State of charge of Li-ion batteries during charging and draining for an 80 percent SOC initiative.

On the other hand, the three-phase converter allows a more uniform distribution of current and reduces fluctuations. Using the latter can also reduce current harmonics and improve the quality and quantity of energy delivered to the battery. Thus, it offers better performance, energy efficiency, and high SOC to maintain the performance specifications. However, it should be noted that the choice of the three-phase interlaced converter depends on the specific system requirements and design constraints.

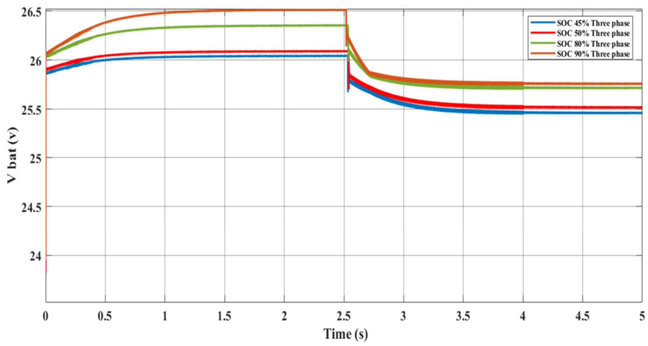

Fig. 6. Three-phase converter battery voltage.

It is crucial to examine some factors to compare the outcomes and functionality of the DC-DC converter interlaced with a parallel MOSFET in two and three phases. Similar benefits are provided by the two layouts, including fewer switching losses and current disturbances due to the distribution of load among the transistors. Nevertheless, these two strategies also differ greatly in important ways:

- The main difference lies in the number of phases used, as this difference can affect the current distribution and stability of the system.
- The number of phases can influence the distribution of current load between the MOSFET in parallel. In the case of the three-phase converter, this number is divided by three. This load distribution can have an impact on conduction losses and system efficiency.
- The number of phases can also influence battery state control. Different initial battery SOC values can affect system dynamics, regulation accuracy, and stability.

To obtain a more profound comprehension of the distinctions between these two scenarios, particular simulations and analyses must be carried out. Three phases provide a more evenly current distribution in the inductors of a three-phase interlaced DC-DC converter. A third of the total current flows through each phase, minimizing imbalances and oscillations amongst the inductors. In addition, proper balancing of the inductor currents helps to reduce the current ripples in the system. Current ripples can cause unwanted electromagnetic disturbances, additional energy losses, and degradation of the overall performance of the converter. It is important to note that balancing inductor currents also depends on the system design, component selection, and control strategy used. Proper design and accurate current regulation can help to improve the equilibration of inductor currents.

The three-phase converter can be marginally more efficient than the two-phase converter due to the ameliorated current distribution. More energy is transmitted to the battery to charge the SOC when the efficiency is higher, since less energy is lost as heat, which may cause the three-phase converter's battery SOC to increase. This leads to the second point, which is the response time: The three-phase converter can also offer a faster response time due to its three-phase switching configuration. The three-phase converter can react more quickly to load changes or battery SOC variations with three switching phases. This allows for more accurate control of the charge and discharge current, which can reduce the time required to reach a SOC target. Consequently, the three-phase converter can charge or discharge the battery faster, resulting in higher battery SOC values in a given time frame.

The employment of three sets of MOSFETs in parallel improves the load and power distribution among the phases in a three-phase interlaced DC-DC converter. Therefore, the system's current distribution improves, and switching losses are reduced. Additionally, the overall conversion efficiency of the three-phase converter might be higher. A more effective converter may extract energy from the power source and transmit it to the battery more effectively during charging or discharging. This indicates that the three-phase converter can charge the battery with less energy loss for the same amount of power supplied by the power source. By reducing energy losses, the three-phase converter can charge the battery more effectively, resulting in a higher SOC. This means that for the same amount of energy provided by the power source, the three-phase converter can store a greater amount of energy in the battery, leading to a higher SOC. It should be noted that additional variables, such as the MOSFETs threshold voltage, the battery control setup, the battery's internal resistance, etc., may also affect SOC. So, when analyzing three-phase converters, it is crucial to consider all of these details.

V. CONCLUSION

This study presented a new modulation (IPWM) on an interleaved bidirectional three-phase DC-DC converter topology to achieve greater efficiency and excellent current distribution between the switches. The inductor current ripple frequency was twice as high as the switching frequency, the battery current ripple frequency was four times higher than the switching frequency, and current ripple cancelation happened at 25% of the duty cycle. In summary, this study demonstrated that the proposed novel modulation of the bidirectional DC-DC converter could be used for both low- and high-power densities.

ACKNOWLEDGEMENT

The authors gratefully acknowledge the approval and support of this study by Grant No. ENGA-2023-12-2236 from the Deanship of Scientific Research at Northern Border University, Arar, Saudi Arabia.

REFERENCES

[1] A. D. Savio and J. A. Vimala, "Development of multiple plug-in electric vehicle mobile charging station using bidirectional converter," *International Journal of Power Electronics and Drive Systems (IJPEDS)*, vol. 11, no. 2, pp. 785–791, Jun. 2020, https://doi.org/10.11591/ijpeds.v11.i2.pp785-791.

[2] N. Mutoh and T. Inoue, "A Control Method to Charge Series-Connected Ultraelectric Double-Layer Capacitors Suitable for Photovoltaic Generation Systems Combining MPPT Control Method," *IEEE Transactions on Industrial Electronics*, vol. 54, no. 1, pp. 374–383, Feb. 2007, https://doi.org/10.1109/TIE.2006.885149.

[3] F. Musavi, M. Edington, and W. Eberle, "Wireless power transfer: A survey of EV battery charging technologies," in *2012 IEEE Energy Conversion Congress and Exposition (ECCE)*, Raleigh, NC, USA, Sep. 2012, pp. 1804–1810, https://doi.org/10.1109/ECCE.2012.6342593.

[4] M. E. Bendib and A. Mekias, "Solar Panel and Wireless Power Transmission System as a Smart Grid for Electric Vehicles," *Engineering, Technology & Applied Science Research*, vol. 10, no. 3, pp. 5683–5688, Jun. 2020, https://doi.org/10.48084/etasr.3473.

[5] I. W. Cox, "Electric vehicle traction control system and method," US9205758B2, Dec. 08, 2015.

[6] D. G. Dorrell, M.-F. Hsieh, M. Popescu, L. Evans, D. A. Staton, and V. Grout, "A Review of the Design Issues and Techniques for Radial-Flux Brushless Surface and Internal Rare-Earth Permanent-Magnet Motors," *IEEE Transactions on Industrial Electronics*, vol. 58, no. 9, pp. 3741–3757, Oct. 2010, https://doi.org/10.1109/TIE.2010.2089940.

[7] S. A. Ahmad Tarusan, A. Jidin, M. L. Mohd Jamil, K. Abdul Karim, and T. Sutikno, "A review of direct torque control development in various multilevel inverter applications," *International Journal of Power Electronics and Drive Systems (IJPEDS)*, vol. 11, no. 3, pp. 1675–1688, Sep. 2020, https://doi.org/10.11591/ijpeds.v11.i3.pp1675-1688.

[8] T. Ahmed, H. Kada, and A. Ahmed, "New DTC strategy of multi-machines single-inverter systems for electric vehicle traction applications," *International Journal of Power Electronics and Drive Systems (IJPEDS)*, vol. 11, no. 2, pp. 641–650, Jun. 2020, https://doi.org/10.11591/ijpeds.v11.i2.pp641-650.

[9] D. Casadei, F. Profumo, G. Serra, and A. Tani, "FOC and DTC: two viable schemes for induction motors torque control," *IEEE Transactions on Power Electronics*, vol. 17, no. 5, pp. 779–787, Sep. 2002, https://doi.org/10.1109/TPEL.2002.802183.

[10] L. Xi, X. Zhang, C. Sun, Z. Wang, X. Hou, and J. Zhang, "Intelligent Energy Management Control for Extended Range Electric Vehicles Based on Dynamic Programming and Neural Network," *Energies*, vol. 10, no. 11, Nov. 2017, Art. no. 1871, https://doi.org/10.3390/en10111871.

[11] N. Priyadarshi, M. S. Bhaskar, P. Sanjeevikumar, F. Azam, and B. Khan, "High-power DC-DC converter with proposed HSFNA MPPT for photovoltaic based ultra-fast charging system of electric vehicles," *IET Renewable Power Generation*, Jun. 2022, https://doi.org/10.1049/rpg2.12513.

[12] Y. Xing, E. W. M. Ma, K. L. Tsui, and M. Pecht, "Battery Management Systems in Electric and Hybrid Vehicles," *Energies*, vol. 4, no. 11, pp. 1840–1857, Nov. 2011, https://doi.org/10.3390/en4111840.

[13] K. Fahem, D. E. Chariag, and L. Sbita, "On-board bidirectional battery chargers topologies for plug-in hybrid electric vehicles," in *2017 International Conference on Green Energy Conversion Systems (GECS)*, Hammamet, Tunisia, Mar. 2017, pp. 1–6, https://doi.org/10.1109/GECS.2017.8066189.

[14] Y. Bian, Y. Zheng, W. Ren, S. E. Li, J. Wang, and K. Li, "Reducing time headway for platooning of connected vehicles via V2V communication," *Transportation Research Part C: Emerging Technologies*, vol. 102, pp. 87–105, May 2019, https://doi.org/10.1016/j.trc.2019.03.002.

[15] A. Flah and C. Mahmoudi, "Design and analysis of a novel power management approach, applied on a connected vehicle as V2V, V2B/I, and V2N," *International Journal of Energy Research*, vol. 43, no. 13, pp. 6869–6889, 2019, https://doi.org/10.1002/er.4701.

[16] X. Li *et al.*, "A Unified Control of Super-capacitor System Based on Bi-directional DC-DC Converter for Power Smoothing in DC Microgrid," *Journal of Modern Power Systems and Clean Energy*, vol. 11, no. 3, pp. 938–949, 2023, https://doi.org/10.35833/MPCE.2021.000549.

[17] K. B. Vikhyath and N. A. Prasad, "Combined Osprey-Chimp Optimization for Cluster Based Routing in Wireless Sensor Networks: Improved DeepMaxout for Node Energy Prediction," *Engineering, Technology & Applied Science Research*, vol. 13, no. 6, pp. 12314–12319, Dec. 2023, https://doi.org/10.48084/etasr.6542.

[18] N. Ding, K. Prasad, and T. t. Lie, "The electric vehicle: a review," *International Journal of Electric and Hybrid Vehicles*, vol. 9, no. 1, pp. 49–66, Jan. 2017, https://doi.org/10.1504/IJEHV.2017.082816.

[19] Q. Yan, B. Zhang, and M. Kezunovic, "Optimization of electric vehicle movement for efficient energy consumption," in *2014 North American Power Symposium (NAPS)*, Pullman, WA, USA, Sep. 2014, pp. 1–6, https://doi.org/10.1109/NAPS.2014.6965467.